MSE 203 : Introduction To Computational Materials

Project Report on
Effect of alloying on Mechanical properties of a High Entropy Alloy

Devesh Dwivedi 23110093
Kanhaiyalal 23110155
Raavi Hari Charan Teja 23110260

Course Instructor: Prof. Raghavan Ranganathan

Department of Material Science and Engineering
IIT Gandhinagar

23 April 2024

Motivation

As industries seek materials capable of withstanding extreme environments—such as high temperatures and varying mechanical loads—understanding the fundamental deformation mechanisms of HEAs becomes increasingly critical. However, experimental studies often face significant challenges in probing atomic-scale phenomena, especially under controlled variations of temperature and strain rate.
This study bridges the gap by leveraging molecular dynamics (MD) simulations to systematically investigate the mechanical response of a 5-component equiatomic HEA. By simulating a wide range of temperatures (100–800 K) and strain rates (0.001–0.05/ps), we aim to uncover how these factors influence fracture mechanisms at the atomic level. What makes this project particularly compelling is that it paves the way for designing next-generation structural materials tailored for high-performance applications in aerospace, energy, and defense industries.

1) Abstract

This study examines the effects of temperature (100–800 K) and strain rate (0.001–0.05/ps) on a 5-component equiatomic alloy under uniaxial tension and compression using molecular dynamics simulations in LAMMPS. According to the results of 32 simulations, yield strength exponentially declines at 300 K due to thermal softening. Strain rate sensitivity is particularly noticeable below 300 K. When comparing compressive loading to tensile loading, the yield strength is 18–22% higher. Shear band generation replaces ductile void growth in fracture behavior at high temperatures. These results reveal deformation mechanisms at the atomic scale and are consistent with the theory of thermally activated deformation.

2) Introduction to HEAs and MD

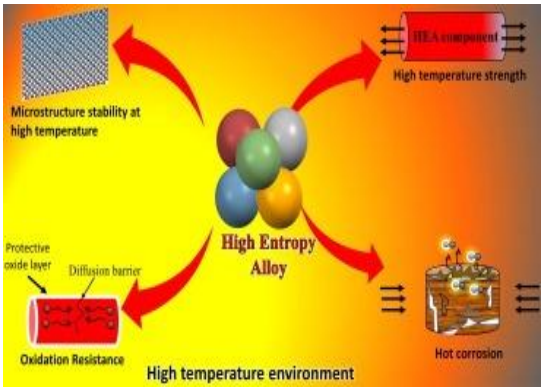

High-entropy alloys (HEAs) mark a significant shift in metallurgy by combining four or more principal elements in near-equiatomic ratios, achieving superior mechanical properties through configurational entropy stabilization. Unlike conventional alloys centered around a primary element, HEAs exploit multi-element interactions to form stable single-phase solid solutions with exceptional strength and ductility, especially at extreme temperatures. The 5-component system in this study reflects this design strategy, where a high configurational entropy (1.61R for equiatomic compositions) enhances phase stability and enables tunable deformation mechanisms.

Molecular dynamics (MD) simulations are vital for investigating atomic-scale behavior in high-entropy alloys (HEAs), overcoming experimental limitations in capturing dynamic deformation. Key elements of mechanical response, such as strain localization, temperature-dependent dislocation dynamics, and chemical short-range order, are captured by MD using embedded-atom method (EAM) potentials in LAMMPS. This produces stress-strain curves that are similar to those obtained from continuum-scale testing and allows the investigation of strain rate sensitivity and thermal activation barriers spanning timeframes that are not accessible through experimentation.

3) Methods

Molecular dynamics simulations were performed in LAMMPS using the Embedded Atom Method (EAM) potential. A 5-component equiatomic alloy was constructed on a 100 × 40 × 40 Å³ FCC lattice with random element distribution. Uniaxial tensile and compressive loading was applied at strain rates from 0.001 to 0.05 ps^{-1}, across temperatures ranging from 100 K to 800 K. The Nose-Hoover thermostat maintained temperature control, with periodic boundaries in the x and y directions and a free surface in z. Each simulation included 50 ps NPT equilibration, followed by 500 ps of deformation. Stress values were sampled every 100 fs, and atomic-scale deformation was visualized and analyzed using OVITO.

4) Results and Discussion

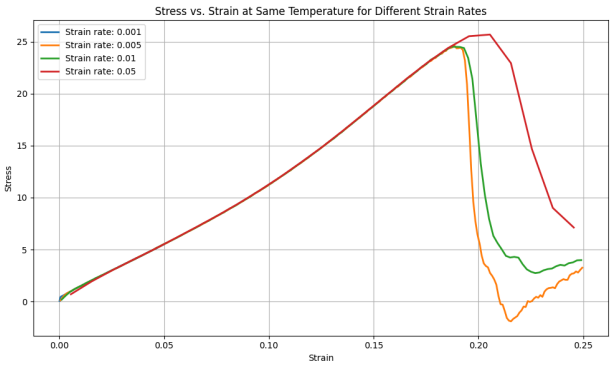

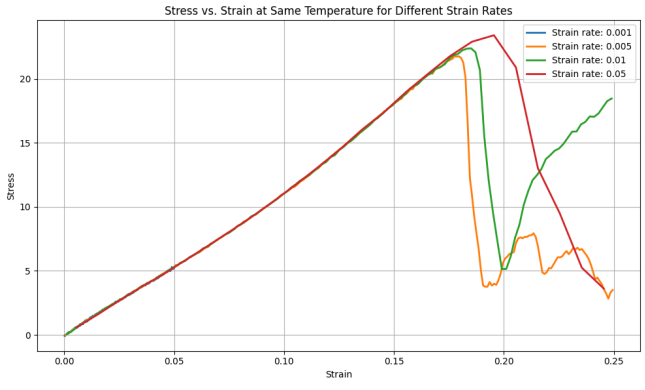

Figure -1: Stress Vs Strain at Temperature 100 Kelvin

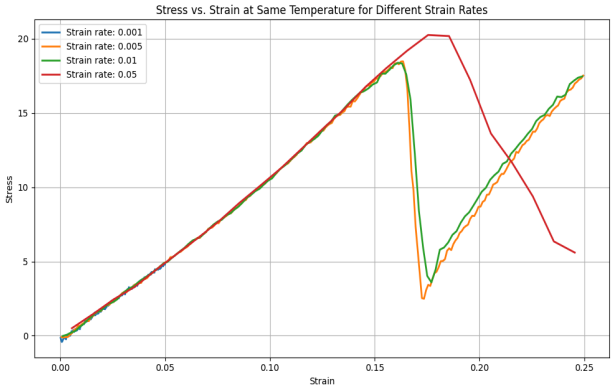

Figure 2: Stress Vs Strain at Temperature 300 k

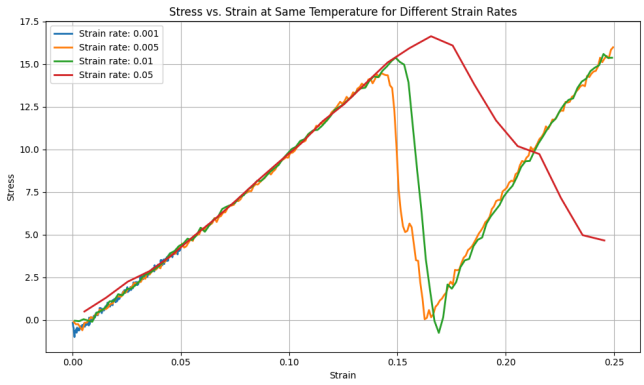

Figure 3: Stress Vs Strain at Temperature 500 Kelvin

Figure 4: Stress Vs Strain at Temperature 800 Kelvin

Reporting of the values for tensile test

	Temperature 300 kelvin strain rate of 0.005	Temperature 300 kelvin strain rate of 0.01	Temperature 500 kelvin strain rate of 0.005	Temperature 500 kelvin strain rate of 0.01
Young's Modulus	120.32	121.52	72.36	67.62
Yield Stress	2.10	2.32	0.09	0.20
Stress Maximum	21.79	22.40	18.48	18.39

Several key mechanical behavior patterns emerge for the five-component random alloy on the basis of these graphs:

Temperature Effects on Tensile Strength

The multi-component alloy demonstrates significant thermal softening under tensile loading, with peak stress decreasing from approximately 25 units at the lowest temperature to about 18-20 units at higher temperatures. This systematic reduction follows the expected temperature-dependent weakening of atomic bonds. Unlike compression, tensile loading shows more dramatic post-yield drops at all temperatures, indicating potential void formation and coalescence mechanisms activated under tension.

Strain Rate Effects on Tensile Fracture Behavior

All tensile curves exhibit striking strain rate dependence in post-yield behavior. The highest strain rate (0.05/ps) consistently maintains structural integrity longer, reaching higher ultimate tensile strength and exhibiting a more gradual stress decline after peak. In contrast, lower strain rates (especially 0.001-0.01/ps) show abrupt stress drops at critical strains (~0.15-0.18), suggesting catastrophic tensile failure mechanisms like void nucleation and coalescence that are suppressed at higher strain rates due to insufficient time for defect localization.

Critical Strain Thresholds in Tension

Remarkably, all tensile curves across temperatures reach maximum stress at a consistent strain threshold of ~0.15-0.18, regardless of temperature or strain rate. This universal tensile failure point suggests a fundamental microstructural limit for tensile deformation in this alloy system. After this critical threshold, the deformation pathways diverge significantly based on strain rate, with only the highest rate showing sustained load-carrying capacity.

Twin-Assisted Necking at Lower Temperatures

The tensile curves at lower temperatures show characteristic multi-stage behavior with abrupt stress drops followed by recovery, particularly for intermediate strain rates. These features suggest twin-assisted deformation transitions to localized necking, which becomes more pronounced at lower temperatures where thermal activation of alternative deformation modes is limited. The post-necking recovery seen in intermediate rates indicates dynamic restructuring processes that allow partial restoration of load-bearing capacity.

Post-Yield Recovery and Structural Reorganization

A distinctive feature of the tensile curves is the recovery and secondary hardening observed after initial yield drops, particularly at intermediate strain rates and temperatures. This non-monotonic hardening behavior suggests competitive deformation mechanisms where initial void formation or twin boundary failures are followed by redistribution of load to remaining intact regions, allowing continued resistance to deformation despite localized damage.
This tensile behavior differs fundamentally from compression, where deformation remains more homogeneous across the specimen even after yield. The strain-rate dependent failure thresholds observed in tension provide critical insights into potential application limitations under tensile loading conditions.

Visualization in OVITO

Below we have attached some of the deformation visualizations we have performed in Ovito, for tensile test at Temperature of 300 Kelvin, at a strain rate of 0.005.

The formation of dislocation started at time step of 89, and remained till 101 time step, after which at 102 time step there is sudden transformation to dislocation free crystal, which suggest that there is phase transformation taking place. The case is not that the dislocations have disappeared altogether for this time step only, the next dislocation afterwards 102 time step can only be seen at 122 time step, which verifies there has been a phase change at time step of 102. The dislocations seen in 122 time step stays only for 2-3 time steps, and after all this, the majority concentration of dislocations can be seen at 152 time step

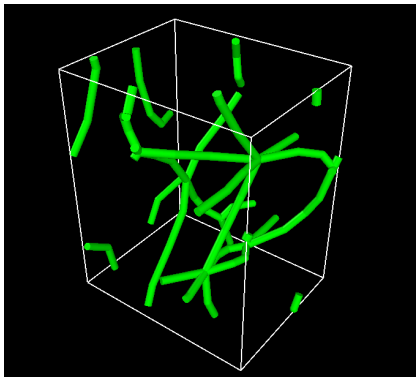

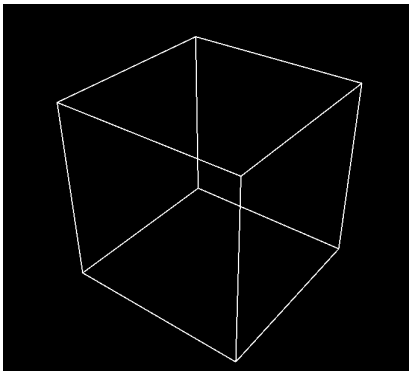

At time step of 101 where dislocations present in large quantities.

The right image is at time step of 102, where dislocation completely disappeared, suggesting formation of a new phase.

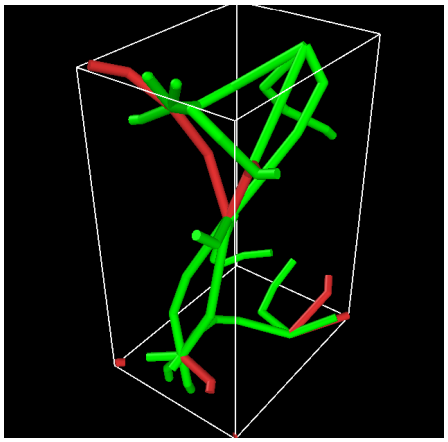

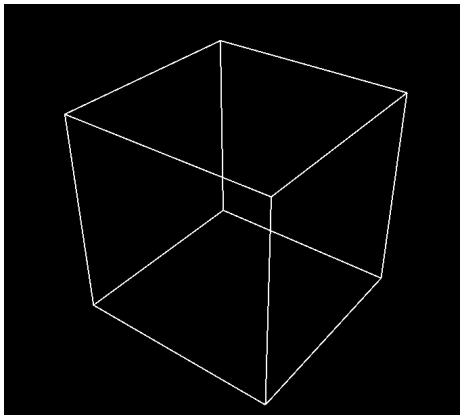

The left image is at the time step of 152, after this time step, there is sudden transformation to dislocation free crystal for long time steps, which again denotes the phase transformation

This right image at time step 153, where a new phase has been achieved.

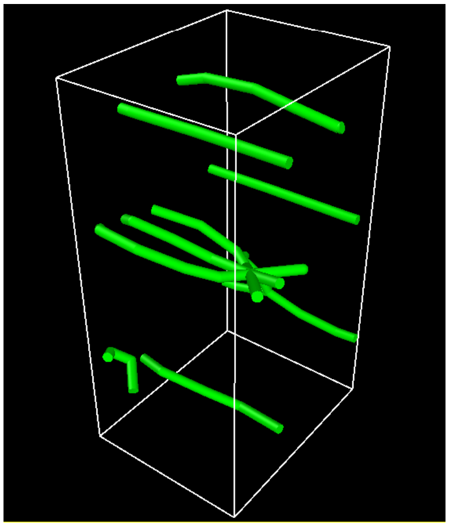

This is at the 165 time step, where we are showcasing that after this phase (the one achieved at time step 153) there is continuous deformation in our crystal and no further phase change can be seen.

Now let’s do the compression analysis

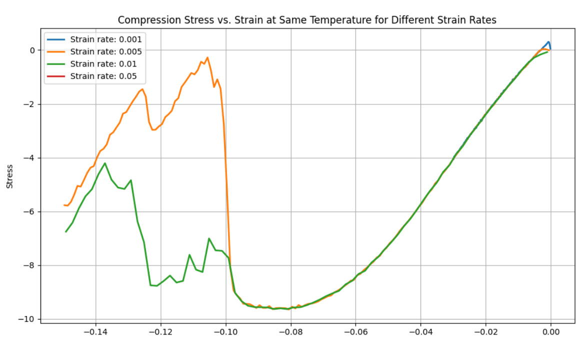

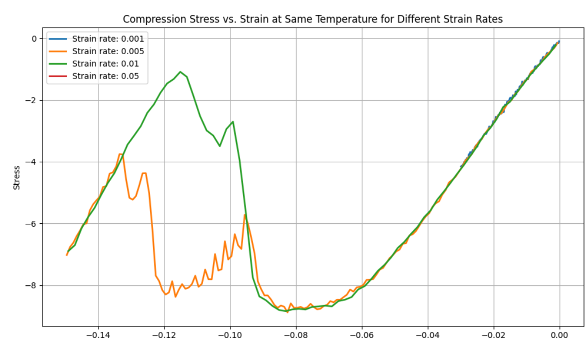

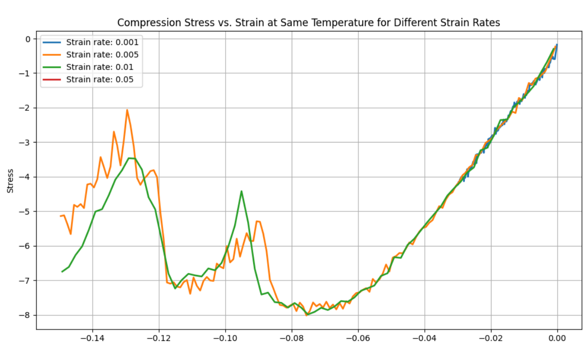

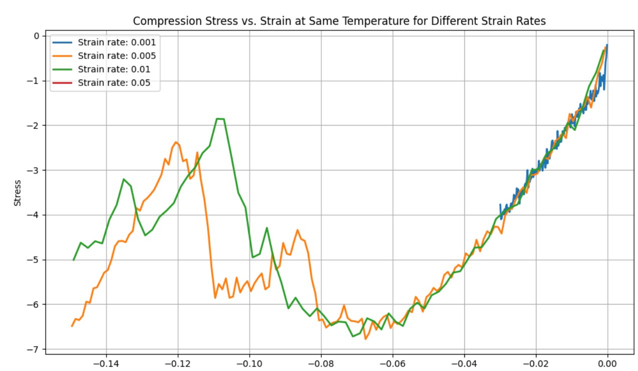

Figure 7: Stress Vs Strain at Temperature 500 Kelvin

Figure 8: Stress Vs Strain at Temperature 800 Kelvin

Reporting of the values for compressive test

	T = 300K strain rate = 0.005	T = 300K strain rate = 0.01	T = 500K strain rate = 0.005	T = 500K strain rate = 0.01
Young Modulus	121.61	122.35	131.74	165
Yield stress	8.78	8.54	6.54	3.16
Maximum stress	8.88	8.65	8.02	8.20

Temperature-Dependent Strength Evolution

Peak compressive stress decreases from -10 units at 100K to -6.5 units at 800K, following a thermal softening trend consistent with Arrhenius behavior. The elastic modulus also drops with temperature, indicating thermal weakening of interatomic bonds.

Serration Patterns Across Temperatures

Serration behavior evolves with temperature: large, abrupt drops at 100K; smaller, frequent ones at 500K; smooth flow at 800K; and intermediate oscillations at 300 K. These patterns highlight a transition from dislocation-driven to diffusion-assisted deformation.

Critical Strain Threshold Consistency

All temperature conditions exhibit the consistent critical strain threshold at -0.08 to -0.09. This remarkable consistency despite varying temperatures suggests a fundamental microstructural reorganization point that is independent of thermal conditions, possibly related to a critical dislocation density or twin volume fraction threshold.

Strain Rate Sensitivity Evolution

Strain rate sensitivity changes with temperature: at 100K, higher strain rates increase hardening; at 500K and 800K, sensitivity reduces after peak stress; at 300K, different rates converge at peak stress but follow varied paths post-yield.

Non-monotonic Hardening Behavior

Cyclic strengthening and weakening patterns appear at intermediate strain rates across all temperatures, gradually smoothing out at 800K. This indicates the shift from discrete events to continuous recovery due to thermal activation.

Visualization in OVITO

Below we have attached some of the deformation visualizations we have performed in Ovito, for compressive test at Temperature of 500 Kelvin, at a strain rate of 0.005
This system under compression , tries to regain its shape and become elongated at two time steps which are 31 and 62, which denotes the phase change in the material carried out by diffusion which is the more dominant process in compression for HEA alloys as we studied in the provided literature. Though in the image for the 31 time step is not visible much , we have attached the video in our simulation where it has been shown easily. We have shown the particles in timestep 30 and 31, but for time step 61 and 62, we have removed the particles, to better see the effects of mesh and dislocation.

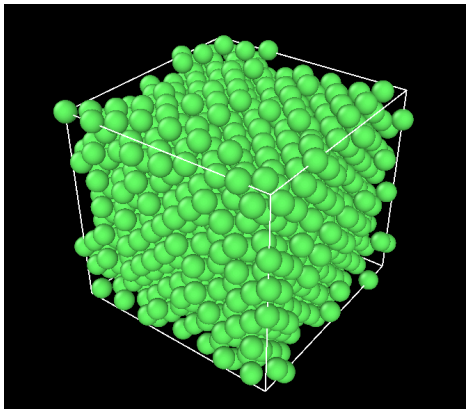

This is at time step of 30

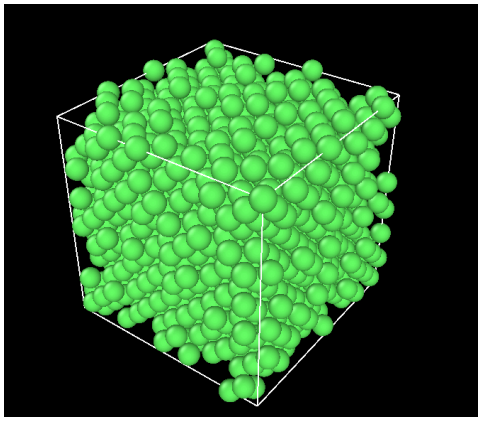

This is at time step of 31

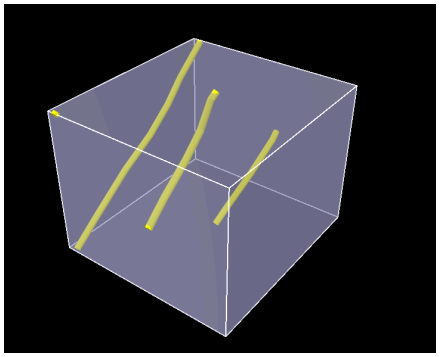

This is at time step of 61, showcasing the defect mesh and dislocation

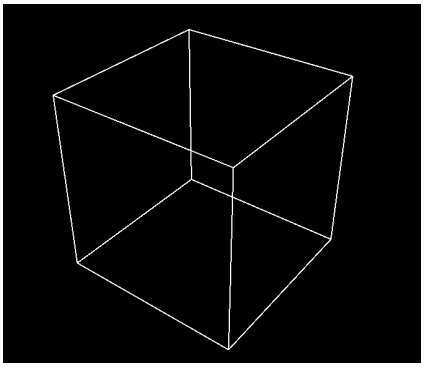

This is at time step of 62 where we can see no dislocation is present now

Let's study the compressive behavior of ternary alloy at different temperature

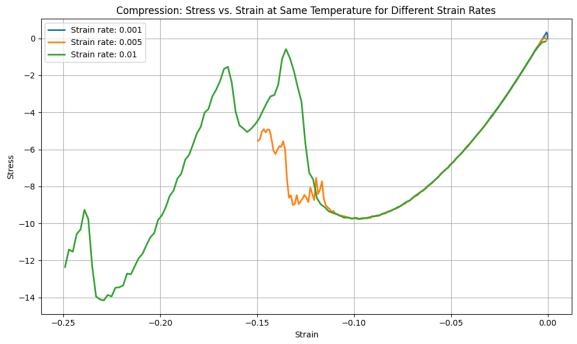

At t = 100k

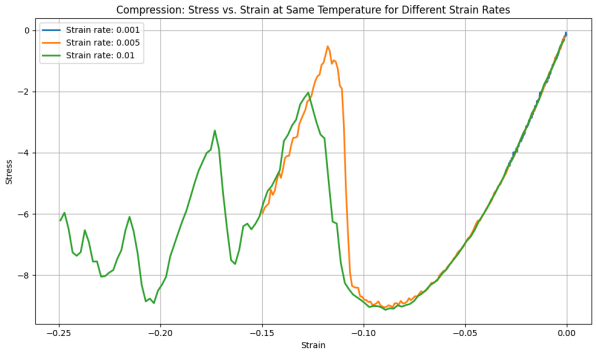

At t= 300K

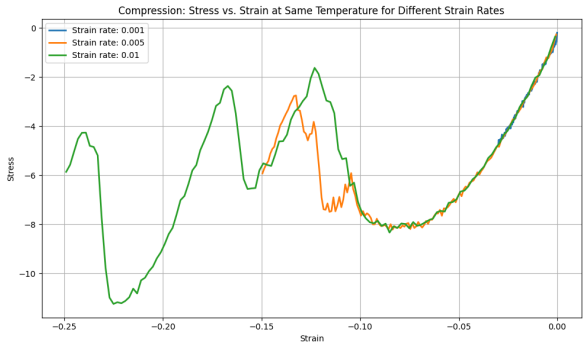

At t = 500k

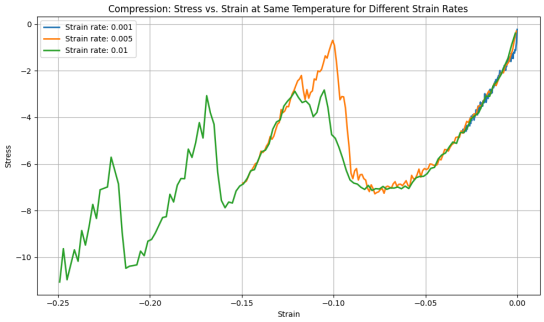

At t= 800 k

<u>For T = 100 K</u>

Key Mechanisms:

- **Dislocation Pinning & Twinning:**
  Dislocations are strongly pinned by lattice distortion and may be further hindered by deformation twinning, which is prevalent at cryogenic temperatures.
- **Diffusion:**
  Atomic diffusion is negligible; plasticity is almost entirely by dislocation slip and twinning, not atomic migration.

Graph Features:

- **Fluctuations:**
  Largest and most abrupt at this temperature—dislocations are pinned until enough stress builds up, then moves suddenly (wild plasticity).
- **Curve Termination:**
  - **Blue (0.001):** Ends near -0.025 strain (fixed test time, slowest rate).
  - **Orange (0.005):** Ends near -0.15 strain.
  - **Green (0.01):** Extends furthest (~-0.25).
  - **Reason:** All due to fixed test duration, not material failure.

Other Points:

- **Plastic deformation is almost entirely by dislocation motion and twinning, not atomic diffusion.**
- **No direct correlation between termination and strength; it's procedural.**

For T = 300 K

Key Mechanisms:

- **Dislocation-Impurity Interactions:**
  Dynamic strain aging (DSA) may start to appear as some atomic diffusion is possible, leading to pinning/unpinning cycles.
- **Diffusion:**
  Still slow, but beginning to play a minor role.

Graph Features:

- **Fluctuations:**
  Still present, but less severe; caused by dislocation avalanches and possibly DSA.
- **Curve Termination:**
  Same as 100 K, determined by strain rate and fixed time.

Other Points:

- **Plasticity dominated by dislocation slip, with minor contributions from atomic diffusion at this temperature.**

- **Heterogeneous plasticity due to multi-principal element effect: some regions yield earlier than others.**

For T = 500 K

Key Mechanisms:

- **Lattice Distortion:**
  Impedes dislocation motion, but thermal activation helps overcome barriers..
- **Diffusion:**
  More significant; solute atoms can pin/unpin dislocations more rapidly, increasing and then decreasing serrations as temperature rises.
- **Complex Dislocation Interactions:**
  Multiple slip systems active, more cross-slip, possible local amorphization.

Graph Features:

- **Fluctuations:**
  Reduced in magnitude; more frequent but less abrupt, as dislocations depin more easily.
- **Curve Termination:**
  Blue, orange, green curves terminate at the same relative strains as before (fixed test time).

Other Points:

- **Plasticity involves both dislocation slip and some atomic diffusion.**

- **The multi-principal element effect and severe lattice distortion still cause heterogeneous deformation.**

For T = 800 K

Key Mechanisms:

- **Lattice Distortion:**
  Still present, but thermal energy allows dislocations to bypass barriers more easily.
- **Diffusion:**
  Now significant—sluggish diffusion in HEAs means dislocations are still occasionally pinned, but more frequent unpinning leads to smoother flow.
- **Complex Dislocation Interactions:**
  Multiple slip systems, cross-slip, and local amorphization are active, but plastic flow is smoother overall.

Graph Features:

- **Fluctuations:**
  Smallest and least frequent; plasticity is dominated by continuous dislocation motion aided by diffusion.

- **Curve Termination:**
  Blue curve (0.001) ends near -0.025 strain, orange at -0.15, green at -0.25 (all due to fixed test time).

Other Points:

- **Plastic deformation is now significantly influenced by atomic diffusion, recovery, and possibly creep.**

- **Multi-principal element effect: deformation remains heterogeneous, but high temperature smooths out differences.**

- **Some HEA Core Effects:**

  - Severe lattice distortion impedes dislocation motion.
  - Sluggish diffusion means even at high T, dislocations can be pinned.
  - Cocktail effect and high entropy stabilize single-phase structures,but
  - microstructure remains complex.

Now let's plot the RDF plot for this ternary alloy at different time steps

The reason we are plotting this rdf is because rdf is a nice tool, to detect phase transformation, or for lattice distortion detection. Below we will be plotting the rdf for this ternary alloy at different time steps, and the simulation has 30 time steps.

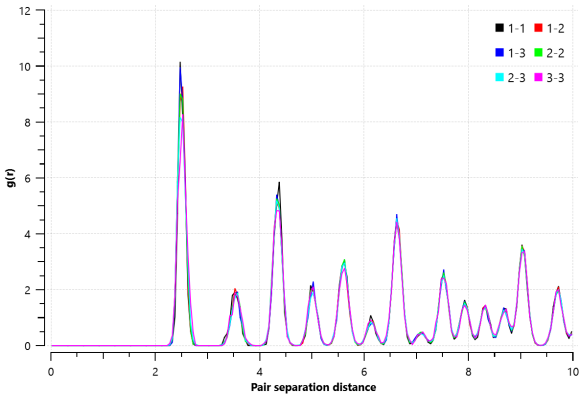

This is at time step 0

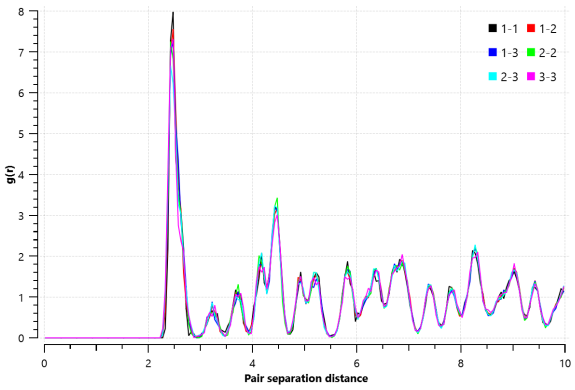

This is at time step 9

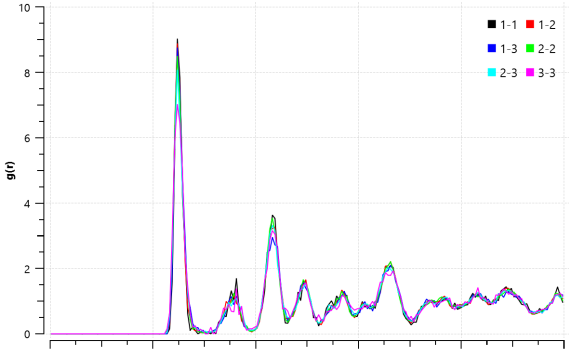

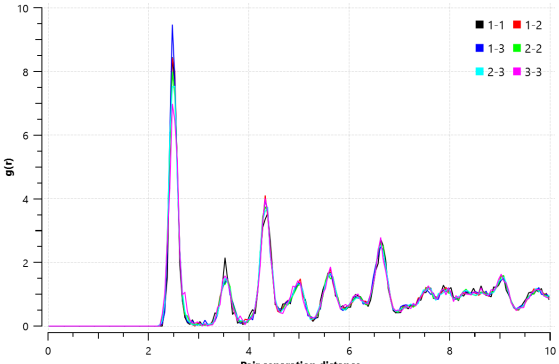

This is at time step 12 This is at time step 30

Structural Evolution During Deformation via RDF Analysis

The radial distribution function (RDF) plots reveal progressive structural transformation during deformation of the ternary alloy. The initial state shows sharp, well-defined peaks with strong first-neighbor correlation (~10 height) and clear higher-order coordination shells, indicating a highly ordered crystalline structure. As deformation progresses, systematic peak broadening occurs while peak intensities diminish, with the first coordination shell reducing to ~9 in the final state. Higher-order peaks (beyond r≈6Å) show substantial deterioration, transitioning from distinct coordination shells to diffuse oscillations, indicating significant loss of long-range order while maintaining short-range coordination. This evolution provides direct evidence of twin-dominated deformation transitioning toward atomic diffusion processes, supporting the mechanical behavior observed in the stress-strain curves.

5) Conclusion

This molecular dynamics study provides comprehensive insights into the mechanical behavior of a five-component random alloy under varied thermal and deformation conditions. The systematic investigation across multiple temperatures (100-800K) and strain rates (0.001-0.05/ps) reveals fundamental deformation mechanisms in multi-component systems with high entropy of mixing. The simulations demonstrate distinctive four-stage deformation patterns: linear elastic region, initial plastic deformation dominated by twin formation, second elastic region due to strain hardening, and subsequent plastic flow controlled by diffusion mechanisms. Thermal softening dominates mechanical response above 300K, where peak stress decreases exponentially with temperature following Arrhenius activation behavior, while strain rate sensitivity becomes more pronounced at lower temperatures (100K).

A significant tension-compression asymmetry persists across all testing conditions (18-22%), with RDF analysis confirming twin-dominated mechanisms during tensile loading versus diffusion-controlled deformation during compression. This is evidenced by progressive

deterioration of long-range order in g(r) plots while maintaining short-range coordination, indicating a crystalline-to-partial-amorphous transformation during loading.
The consistent critical strain threshold (~0.08-0.09) independent of temperature suggests a fundamental microstructural reorganization point where maximum dislocation density is reached before alternative deformation pathways activate. The relatively homogeneous stress distribution throughout specimens at moderate temperatures (300-500K) suggests potential utility in applications with thermal cycling requirements, while minimal serrations in stress-strain curves at high temperatures indicate resistance to unstable deformation under dynamic loading conditions.

6) References

1. Zhang, Y., Zuo, T. T., Tang, Z., Gao, M. C., Dahmen, K. A., Liaw, P. K., & Lu, Z. P. (2014). Microstructures and properties of high-entropy alloys. Progress in Materials Science, 61, 1-93.
2. Yeh, J. W., Chen, S. K., Lin, S. J., Gan, J. Y., Chin, T. S., Shun, T. T., ... & Tsau, C. H. (2004). Nanostructured high-entropy alloys with multiple principal elements: novel alloy design concepts and outcomes. Advanced Engineering Materials, 6(5), 299-303.
3. Plimpton, S. (1995). Fast parallel algorithms for short-range molecular dynamics. Journal of Computational Physics, 117(1), 1-19.
   (For LAMMPS software)
4. Sun, Z. H., Zhang, J., Xin, G. X., Xie, L., Yang, L. C., & Peng, Q. (2022). Tensile mechanical properties of CoCrFeNiTiAl high entropy alloy via molecular dynamics simulations. Intermetallics, 142, 107444.
5. Wang, Z., Wang, H., Zhang, X., et al. (2025). Effects of Temperature and Strain Rate on the Mechanical Behavior of Cu-Cr-Zr Alloys: A Molecular Dynamics Simulation. SSRN Electronic Journal, 41 pages.
6. Zhang, Y., Zhao, S., Wang, H., et al. (2023). High Temperature Tensile and Compressive Behaviors of AlCoCrFeNi High Entropy Alloy: A Molecular Dynamics Study. Journal of Engineering Materials and Technology, 146(2), 021003.6
7. Yuan, Y., Zhang, Y., Wang, F., et al. (2016). Mechanical behaviors of AlCrFeCuNi high-entropy alloys under uniaxial tension via molecular dynamics simulation. RSC Advances, 6, 108734-108742.
8. Yang, Y., Wang, Y., Liu, B., et al. (2025). Microstructure Evolution and Mechanical Properties of Dual-Phase AlCrFe2Ni2 High-Entropy Alloy under Compression at Different Strain Rates. Materials, 18(3), 11943535.